12WCEE 2000

CORRELATION OF NONLINEAR DISPLACEMENT RESPONSES WITH BASIC CHARACTERISTICS OF EARTHQUAKE MOTION

Yukiko NAKAMURA[1] And Toshimi KABEYASAWA[2]

SUMMARY

Responses of linear and nonlinear systems are correlated with basic characteristics of earthquake motion, which are supposed to be given as the amplitudes and the phases of Fourier spectrum. By assuming the phase difference spectrum in Fourier transform a normal probability curve, the standard deviation of which correlates to the duration of the earthquake, expected value of time-history response to earthquake can be formulated. The effect of damping on the linear response spectrum can be obtained based on this formula. Nonlinear displacement responses to earthquakes can be simulated based on instantaneous balance of input energy and dissipated energy. The input energy can be approximated from linear response spectrum, whereas the energy dissipation capacity and the equivalent period of vibration depend on the path of the hysteresis relations. The peak displacement ratios, which are the ratios of maximum displacement to previous peak displacement during nonlinear response, are defined to represent the hysteretic path. The ratios can also be related to the phase difference spectrum. Estimation of the nonlinear response from an equivalent linear system in capacity-demand diagram can be improved using the peak displacement ratios approximated from the duration of motion.

INTRODUCTION

In displacement-based seismic design, the design criterion is to be that the response of structure shall be less than the limit state, given in terms of story drift or member deformation, such as ultimate deformation capacity of yielding members. To develop the rational design criterion, general correlation must be derived between the inelastic response and characteristics of design earthquake. Here, the basic characteristics of the earthquake are supposed to be given as the amplitudes and the phases of Fourier spectrum. Fourier amplitudes correspond to the total input energy to the undamped system in terms of velocity. On the other hand, the phase angles have been assumed in practical design as random or peculiar to the recorded motion, the effect of which on the response has not yet been studied enough.

The purpose of the study is to analyze the time-history responses based on the characteristics of the earthquake motion. A mathematical formula is given to calculate the expected value of time-history response of the linear damped system under the earthquake motion characterized as above. The results may be useful as the theoretical backgrounds for the effect of damping on the response spectrum, or the peak displacement ratios, which can be used for a rational estimation of nonlinear responses.

CHRACTERISTICS OF INPUT EARTHQUAKE MOTIONS

Earthquake motions used in this study are listed in Table 1. Non-stationary waves can be expressed using the Fourier transform as Fourier amplitudes and phase difference spectrum. It has been pointed out theoretically that the phase difference spectrum is in good correlation with the time-history of the acceleration waveform. Therefore, the deviation of the spectrum may be used to express the duration of the earthquake. Here, the duration time t_0 is defined from 5% to 95% of the time history of the square of the acceleration, called frequency

[1] *Dept of Civil Engineering and Architecture, Niigata University, Niigata, JapanEmail: nakamura@eng.niigata-u.ac.jp*
[2] *Earthquake Research Institute, University of Tokyo, Tokyo, JapanEmail: kabe@eri.u-tokyo.ac.jp*

ensemble work, which corresponds to the work done to the system integrated in the domain of frequency. The duration times calculated for the earthquakes are shown in Table 1, with moment magnitudes of the source for the earthquakes after 1981 or the surface wave magnitudes before 1980. The time-history accelerations are shown in Figure 1.

The relations between the duration and the magnitudes were plotted in Figure 2. Simple empirical equations for the relations [Dobry, 1978][Trifunac, 1975] gives fair approximates for the defined duration. The Fourier

Table 1: List of Earthquake Motions.

Abbreviation	Earthquake	Site	Component	Date of occurrence	Magnitude	Amax(gal)	Duration(s)
elcns	Imperial valley earthquake	El Centro	NS	May 18,1940	7.1	341.7	24.4
taftse69	California earthquake	Kern county	S69E	Jul 21,1952	7.8	175.9	28.9
hacew	Tokachi-Oki	Hachinihe Harbor	EW	May 16,1968	8.2	182.9	24.4
pacs74w	San Fernando earthquake	Pacoima Dam	S74W	Feb 9,1971	6.6	1054.	7.28
tohns	Miyagi-ken-Oki	Tohoku University	NS	Jun 12,1978	7.6	258.2	19.5
sctew	Mexico	SCT1	EW	Sep 19,1985	8.0	167.9	38.9
ksrew	Kushiro-Oki	Kushiro Meteorological Observatory	EW	Jan 15,1993	7.6	711.4	19.3
sylew	Northrige earthquake	Sylmar county hosp.	EW	Jan 17,1994	6.7	826.7	5.34
kobns	Hyogo-ken-Nambu	Kobe Meteorological Obsevatory	NS	Jan 17,1995	6.9	820.6	8.38
fkin30w	Hyogo-ken-Nambu	Ohsaka Gas Fukiai Station	N30W	Jan 17,1995	6.9	802.0	6.76
newrc1	NewRC Artificial	--	--	--	--	394.6	29.6
newrc2	NewRC Artificial	--	--	--	--	407.2	78.5

angles of the two adjacent components in the Fourier decomposition, is idealized as a normal distribution curve. Figure 3 shows examples of the correlation between the phase difference spectrum and the acceleration amplitude has been investigated so far, whereas the effect of the phase on the response has not been studied

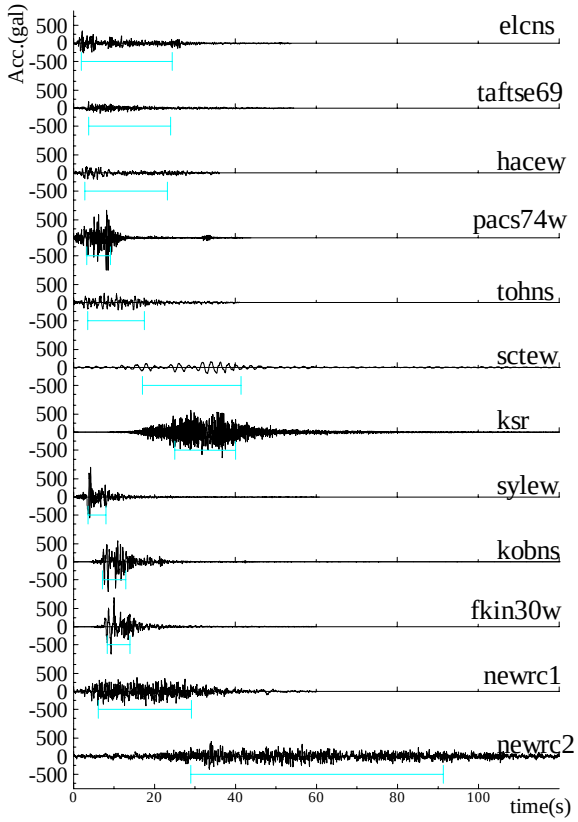

Figure 1: Time-history of accelerams

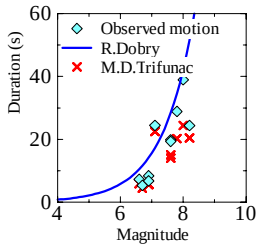

Figure 2: Duration and magnitudes of the earthquakes

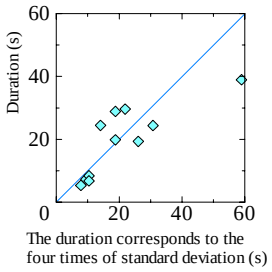

Figure 4: Duration and deviation of the phase difference spectrum

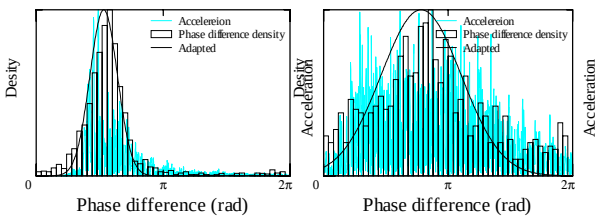

(a) fkin30w (b) newrc1

Figure 3: Probability density of the phase difference spectrum, idealized normal distribution and acceleration wave

much. In the following study, the phase different spectrum, which is defined as the difference between the phase waveform for fkin30w and newrc1. The normal distributions fitted by the least square method are also shown in the figure. The standard deviation of the normal distribution is larger for the earthquake with the longer duration. The distribution of the phase difference spectrum has been verified theoretically to be similar to the envelope shape of the time-history of the original acceleration wave[Ohsaki, 1978]. In other words, the standard deviation of the phase difference spectrum corresponds to the duration of the earthquake motion. As shown in Figure 4, the duration corresponds to the four times of the standard deviation of the idealized normal distribution for the phase difference spectrum.

EXPECTATION OF RESPONSE TIME-HYSTORY FROM PHASE DIFFERENCE SPECTRUM

Expected value of the responses of the linear system with viscous damping was formulated as the superposition of the theoretical transient responses to the decomposed Fourier sinusoidal waves as follows. Earthquake acceleration is decomposed into the Fourier formula as the sum of cosine waves of Nf=N/2+1 as equation(1).

$$\ddot{y}_0(t) = \sum_{k=1}^{Nf} a_k \cos(\omega_k t + \phi_k) \tag{1}$$

$$p(\Delta\phi) = \frac{1}{\sqrt{2\pi}\sigma} \exp\left(-\frac{(\Delta\phi - \mu)^2}{2\sigma^2} \right) \tag{2}$$

where $\phi_k = \sum_{j=1}^{k} \Delta\phi_j$, φ_k : phase angle of the k-th component, $\Delta\varphi_k$: *k-th* phase difference (=φ_k-φ_{k-1}), $\ddot{y}_0(t)$: acceleartion of the motion, $\omega_k \left(= \sqrt{\frac{2\pi k}{N\Delta t}} \right)$: frequency of k-th component in the Fourier transform, N : total number of earthquake data, Δ□ : time increment of earthquake data, and $p(\Delta\phi)$: probability density function of the phase difference spectrum.

It is assumed here that the Fourier amplitudes of the acceleration a_k are invariant and unity to investigate only the effect of phase difference spectrum. Also in the range out of 0 through 2π, the density spectrum is assumed to be negligibly small. Then the input acceleration of *k*-th component is expressed as equation (3).

$$\ddot{y}_{0k}(t) = \cos(\omega_k t + \phi_k) \tag{3}$$

Therefore, the transient response of the system with fundamental frequency ω and damping coefficient h to above component can be formulated as equation (4):

$$\dot{y}_k(t,h) = \Re\left[A_0 \left\{ i\Delta\omega k e^{\Delta\omega kpt} + e^{-h\omega t}(C_1 e^{i\sqrt{1-h^2}\omega t} C_2 e^{-i\sqrt{1-h^2}\omega t}) \right\} e^{i\phi_k} \right] \tag{4}$$

where, $A_0 = \frac{-(\omega^2 {\omega_k}^2 - 2ih\omega\omega_k)}{(\omega^2 {\omega_k}^2)^2 + (2ih\omega\omega_k)^2}$, $C_1 = \frac{1}{2\sqrt{1-h^2}} \left(h\omega_k - \omega - i\omega_k \sqrt{1-h^2} \right)$, $C_2 = \frac{1}{2\sqrt{1-h^2}} \left(h\omega_k - \omega + i\omega_k \sqrt{1-h^2} \right)$, h is viscous damping coefficient of the system, ω is fundamental frequancy of the system. The response to the acceleration $\ddot{y}_0(t)$ can be expressed as equation (5) as the sum of all the components from 1st to Nf-th:

$$\dot{y}(t,h) = \sum_{k=1}^{Nf} \dot{y}_k(t,h) \tag{5}$$

Expected value of the average of the time-history response considering desnsity function of the phase spectrum can be expressed as equation (6):

$$E[\dot{y}(t,h)] = \int_{-\infty}^{\infty} \cdots \int_{-\infty}^{\infty} \{\dot{y}(t,h)\} \prod_{s=1}^{Nf} p(\Delta\phi_s) d\Delta\phi_1 \cdots d\Delta\phi_{Nf} \tag{6}$$

And, the variance of the response is in the following equation(7), from which the envelope curve of the response can be derived as its square root:

$$Var[\dot{y}(t,h)] = \int_{-\infty}^{\infty}\cdots\int_{-\infty}^{\infty}\{\dot{y}(t,h)\}^2\prod_{s=1}^{Nf}p(\Delta\phi_s)d\Delta\phi_1\cdots d\Delta\phi_{Nf} - E[\dot{y}(t,h)]^2 \quad (7)$$

Calculated envelope curves for the systems with damping coefficients of 5, 10, 15 and 20 percent of critical are shown in Figure 5. The values of the standard deviation of the phase difference spectrum are 0.34π and 1.01π for Fukiai and NewRC1 respectively.

EFFECT OF DAMPING ON RESPONSE SPECTRUM

Fourier amplitude spectrum is similar to the velocity response spectrum without damping, which is also correlated to the total input energy spectrum in terms of velocity. In case of the response of the system with higher damping coefficient, the total input energy is invariant but smoothed whereas the velocity response is smaller. The effect of damping on the response has been approximated empirically in practice and research, so that the basic characteristics, for example the phase spectrum, are not reflected in the approximation. However, the effect of damping on the response is apparently different, for example, in the cases of far-field and near-field earthquakes. The relationship between the fundamental frequency of the system and the duration of the earthquake need be investigated.

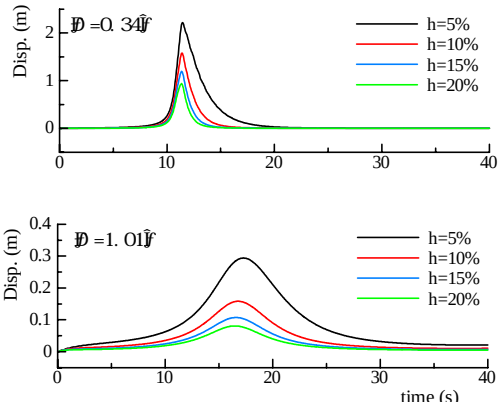

Figure 5: Expected envelope of response time-history

The effect of damping can be formulated based on the power spectrum if the input wave is assumed as a white noise, which is basically determined by the duration of the input wave. Expected constant stable response to the white noise of the duration t_1 is expressed as equation (8), from which the effect of damping on the response is formulated as equation (9):

$$\sigma_y^2 = \frac{S_0}{4h\omega_0^2}\left[1-e^{-2h\omega_0 t_1}\right] \quad (h\neq 0) \quad (8)$$

$$\sigma_y^2 = \frac{S_0 t_1}{2h\omega_0^2} \quad (h=0)$$

$$D_h(h) = \frac{S_V(h)}{S_V(h=0.0)} = \sqrt{\frac{1-e^{-2h\omega_0 t_1}}{2h\omega_0 t_1}} \quad (9)$$

where, σ_y^2 : expected square average of response displacement, S_0 : power spectrum density, t_1 : duration of the white noise, h : damping coefficient, ω_0 : fundamental frequency. The duration of earthquake t_0 must be converted into the equivalent duration in above formula. The equivalent duration t_1 for above equation (9) is derived as $t_1=t_0/4$ empirically so that the reduction from the equation (9) roughly agrees with the calculated responses of the damped system. Examples are shown in Figure 6.

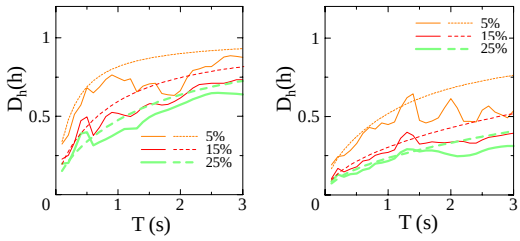

(a) fkin30w (b) newrc1

Figure 6: Reduction ratio of damped response to undamped response and estimation from equivalent white noise

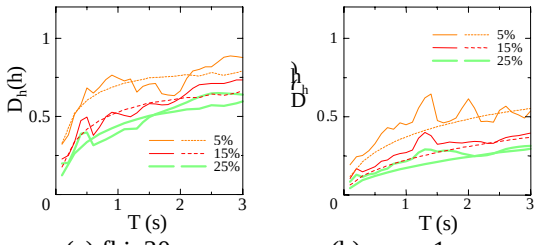

(a) fkin30w (b) newrc1

Figure 7: Reduction ratio of damped response to undamped response and estimation from the phase difference spectrum

Although above formula is simple and practical, the equivalent duration was determined empirically without theoretical background. The time-history

response derived from the phase difference spectrum in the previous section can be used to correlate the effect of damping with the duration of the earthquake. The effect of damping can be formulated as equation (10), only by idealizing the phase difference spectrum as a normal distribution curve:

$$D_h(h) = \frac{S_V(h)}{S_V(h=0.0)} = \frac{Var\left[\dot{y}(t,h)\right]_{\max}}{Var\left[\dot{y}(t,0)\right]_{\max}} \tag{10}$$

The effect of damping on the response derived from above formula as response expectations is shown in Figure 7 for Fukiai and NewRC motions. As shown in the figure, good estimates can be derived theoretically based on the phase difference spectrum or the duration of the earthquake. The reduction of response estimated from above equation is apparently greater than the reduction estimated based on white noise (equation(9)) assuming the equivalent duration of $t_0/4$. Therefore, the equivalent duration longer than $t_0/4$ may be assumed to fit above theory. The response under the actual earthquake is scattering because the phase difference spectrum is not normal distribution and Fourier amplitude is not constant through frequency. The method gives theoretical and smoothed expectation, although it takes a lot of computation time, which may be a theoretical background to the equivalent duration empirically determined based on the white noise.

PEAK DISPLACEMENT RATIO

Input and dissipated energy in the hysteretic damping system is balanced during the response to earthquake motions. In the past studies[Nakamura and Kabeyasawa, 1996], maximum response displacement of hysteretic damping system can fairly be correlated to the instantaneous input energy during the unit time in proportion to the equivalent period of inelastic system. Input energy can be evaluated relatively stable and constant, although it depends on the equivalent period. Also, the input energy to the inelastic system can be correlated to the linear response spectrum. On the other hand, the energy dissipation capacity depends on the hysteretic relations of the system, especially at the latest moment when the maximum displacement occurs.

For example, it is clearly different in the cases that the amplitude increases symmetrically and gradually with cyclic vibration and that the inelastic displacement increases rapidly in one direction. Figure 8 shows the hysteretic response of an inelastic system under NewRC and Fukiai motions. As shown in Figure 8(a) under Fukiai motion, i.e., a near-field motion, the displacement response increases rapidly up to maximum displacement in one cycle, whereas under NewRC motion in Figure 8(b), the response gradually increases with cyclic excitations. To differentiate these types of responses, the index of peak displacement ratio is proposed which is defined as the ratio of the peak displacement in the previous half- or one-cycle to the maximum displacement as follows:

$$\gamma_{1/2} = D_{\min} / D_{\max} \tag{11}$$

$$\gamma_1 = D_{pre} / D_{\max}$$

where, $D_{\max}$: maximum response displacement, $D_{\min}$: half-cycle previous peak displacement in the opposite direction, D_{pre}: one-cycle previous peak displacement in the same direction

Figure 9 shows the peak displacement ratios γ_1 $\gamma_{1/2}$, calculated from responses of various nonlinear systems under NewRC and Fukiai motions. The ratios are plotted in relation to the equivalent period in horizontal axis, which is calculated from the secant stiffness from the origin to the maximum response displacement. The hysteresis rule of the systems is Takeda model, the yield strength of which is selected under each motion so that the nonlinear maximum response displacement of the systems attains the ductility factor of 2, 4, or 9. The

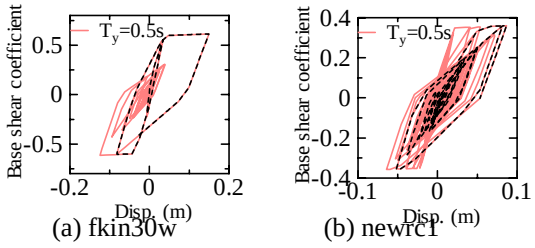

(a) fkin30w (b) newrc1

Figure 8: Examples of hysteretic responses

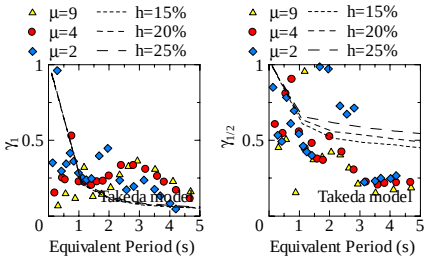

(a) fkin30w

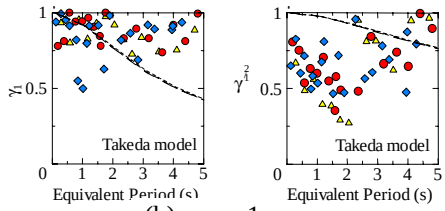

(b) newrc1

Figure 9: Peak displacement ratios

peak displacement ratios are apparently different between the responses under the two motions. They depends on the equivalent period of the system: the ratios are higher under NewRC motion with long duration and lower under Fukiai motion with short duration, which reduce with the elongation of the equivalent period.

The peak displacement ratios can also be derived theoretically from the expectations of time-history response. The ratios calculated from the expectations are plotted in Figure 9 with dotted lines, which conform to the observed relations that the ratios becomes lower with the elongation of the equivalent period and under the motion with short duration. The method gives a theoretical background for the peak displacement ratios. However, it requires too heavy calculations. Therefore, the ratios are formulated by simplifying the time-history of the input energy, as shown in Figure 10, using the duration, on the assumption that:

(1) Instantaneous input energy is the maximum at the middle point of the defined duration of motion.
(2) The maximum instantaneous energy is four times the average energy (two times in terms of velocity), which is defined as the total energy divided by the duration of the motion[Nakamura and Kabeyasawa, 1998].
(3) The maximum displacement occurs at the maximum instantaneous energy.
(4) The peak displacement ratios is in proportion to the maximum input energy, from which γ is given by the following equation, using the duration t_0 and the equivalent period Te,

$$\gamma = \frac{t_0/2 - T_e}{t_0/2 + T_e} = \frac{t_0 - 2T_e}{t_0 + 2T_e} \tag{12}$$

where, t_0 is the duration of motion, T_e is equivalent period

ESTIMATION OF NONLINEAR DISPLACEMENT RESPONSE

To estimate nonlinear and dynamic response to earthquake motions, a simple equivalent linearization is practical using pushover analysis and capacity-demand diagram. As shown in Figure 11, equivalent load-deformation curve of reduced single-degree-of-freedom system from the pushover analysis is plotted on S_A-S_D diagram, namely acceleration-displacement diagram. Then, the nonlinear dynamic response can be estimated to be the crossing point of the capacity curve and the demand curve, where the substitute damping of the hysteretic system is equal to that of the demand curve, i.e., the elastic response spectrum of the motion. It should be noted that the equivalent fundamental period of the hysteretic system is simply and implicitly assumed to correspond to the secant stiffness starting from the origin to the estimated maximum inelastic response.

The accuracy of above method diagram is investigated for the responses of the nonlinear systems with hysteresis rules of Takeda-model, Takeda-Slip model and Bilinear model as shown in Figure 12. The marks of rectangle, triangle or circle are the responses calculated from inelastic system, which attain ductility levels of 2, 4, and 9, which are plotted at the corresponding strength(S_A) and response displacement(S_D). If the estimation method is appropriate, these responses are plotted on the demand curves with the corresponding damping coefficient. A fair correlation is observed only in the case of Takeda model under the artificial design motion of NewRC as shown in Figure 12 (a), in which stationary responses are dominant. In the other cases under recorded motions,

the estimation is much worse in general, an example of which is shown in Figure 12 (b) under Fukiai Staion record (N30W) during 1995 Hyogoken-Nanbu Earthquake. The estimated responses by capacity-demand diagram as the crossing points are compared with the calculated under NewRC and Fukiai motions, as shown in Figure 13. The accuracy is not satisfactory. For example, when the inelastic displacement increases rapidly under near-field earthquake motion, the estimation could be smaller than the calculated.

If the displacement increases symmetrically and gradually with cyclic vibration, then the hysteretic damping in stationary behavior and the secant stiffness to the maximum displacement can be assumed in the estimation. On the other hand, if the inelastic displacement increase rapidly in one direction under relatively short earthquake motion, in other words, the peak displacement ratio is small, then the equivalent fundamental period should be assumed shorter and the energy dissipation capacity should be corrected considering the hysteresis path. In such case, the equivalent stiffness is defined here from the half-cycle previous peak to the maximum peak displacement, as shown in Figure 14. Equivalent viscous damping factor is also defined as the hysteretic damping for the half cycle as shown in the figure. The capacity-demand diagram method was modified using above equivalent period and damping on the assumption that the peak displacement ratio was given by equation (12) based on the duration of the earthquake. The estimated displacement and maximum response displacement under NewRC and Fukiai motion are shown in Figure 15, which give better estimation than those by the simple capacity-demand diagram method. the estimation is much worse in general, an example of which is shown in Figure 12 (b) under Fukiai Staion record (N30W) during 1995 Hyogoken-Nanbu Earthquake. The estimated responses by capacity-demand diagram method.

CONCLUSIONS

Expected value of time-history response can be formulated by assuming the phase difference spectrum in Fourier transform of earthquake waves as a normal probability curve. The effect of damping on the linear response spectrum can be obtained based on this formula, which should be correlated to the duration of earthquake in demand spectrum. The peak displacement ratios, which are the ratio of maximum displacement to previous peak displacement during nonlinear response, can also be calculated theoretically based on above formula from the phase difference spectrum. Estimation of the nonlinear response from an equivalent linear system in capacity-demand diagram can be improved using the peak displacement ratios approximated from the duration of motion.

REFERENCES

Dobry, R. Idriss, I. M. and E. Ng, (1978), “Duration chracteristics of horizontal components of strong-motion earthquake records”, *Bulletin of Seismological Society of America*, Vol.68, No.5, pp1487-1520.

Nakamura, Y. and Kabeyasawa, T., (1996), “Estimation of Maximum Displacement Response of Reinforced Concrete Structures Based on Energy Input Rate Spectrum”, *Transactions of the Japan Concrete Institute*, Vol. 18, pp205-212.

Nakamura, Y. and Kabeyasawa, T., (1998), “Estimation of Maximum Displacement Response of Reinforced Concrete Structures”, *Proceedings of the Tenth Japan Earthquake Engineering Symposium*,

Ohsaki, Y., Iwasaki, R., Ohkawa, I. and Masao, T., (1978), “A study phase characteristics of earthquake motions and its application”, *Proceedings of the Fifth Japan Earthquake Engineering Symposium*, pp201-208

Trifunac, M. D. and Brady, A. G. (1975), “A study on the strong earthquake ground motion”, *Bulletin of Seismological Society of America*, Vol.65, No.3, pp581-626.

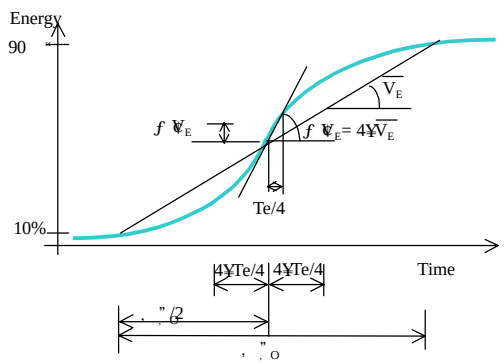

Figure 10: Simplified model of energy input time-history

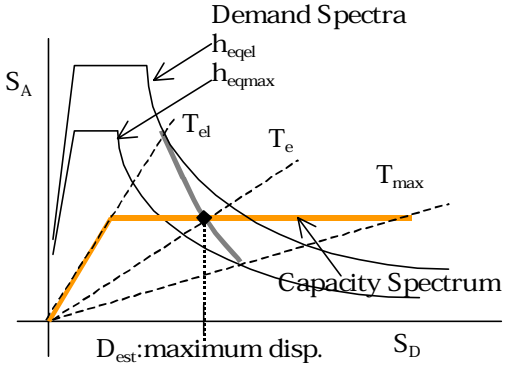

Figure 11: Capacity-demand diagram method

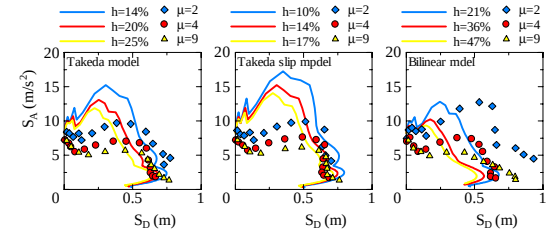

(a) fkin30w

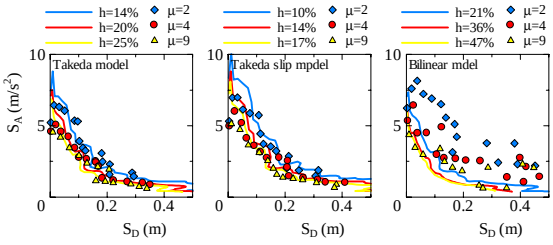

(b) newrc1

Figure 12: Responses of nonlinear system and demand curves in S_A-S_D format

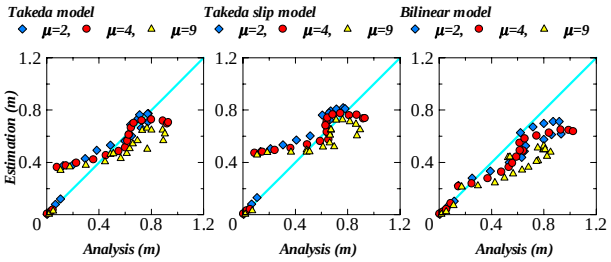

(a) fkin30w

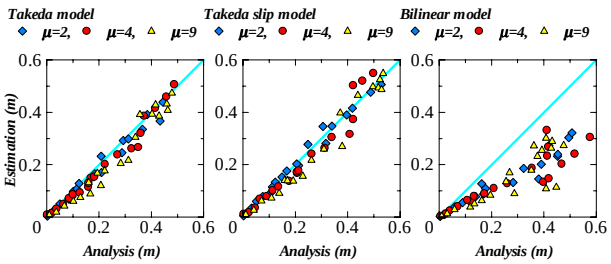

(b) newrc1

Figure 13: Estimation by capacity-demand diagram with calculated nonlinear responses

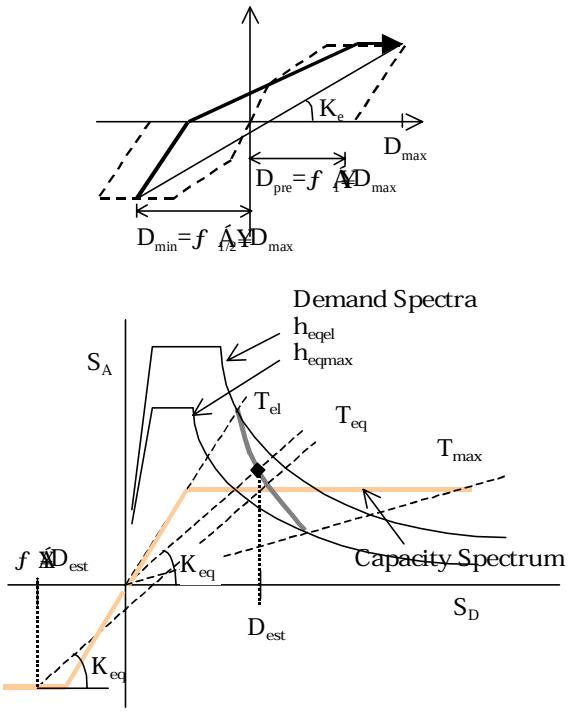

Figure 14: Modified capacity-demand diagram method using peak displacement ratios

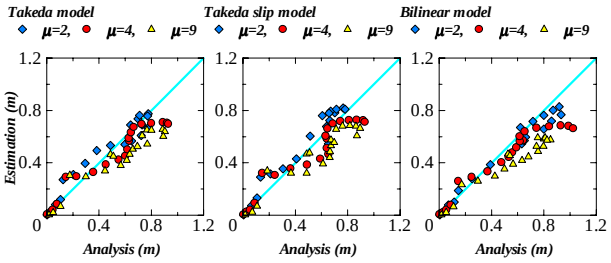

(a) fkin30w

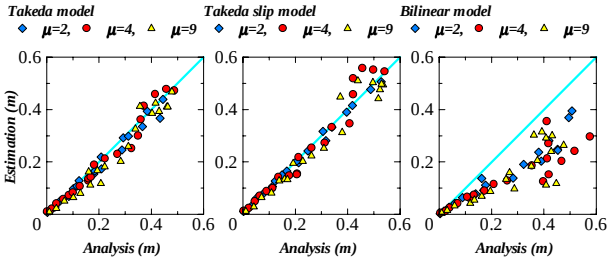

(b) newrc1

Figure 15: Modified estimation with calculated nonlinear responses